Journal of Applied Polymer Science

Thermal Properties and Crystallization Behavior of Fractionated Blocky and Random Polyhydroxyalkanoate Copolymers from Mixed Microbial Cultures

Bronwyn Laycock,[1] Monica V. Arcos-Hernandez,[2] Alexandra Langford,[1] Jessica Buchanan,[1] Peter J. Halley,[1] Alan Werker,[2] Paul A. Lant,[1] Steven Pratt[1]

[1]School of Chemical Engineering, University of Queensland, St Lucia, Queensland 4072, Australia

[2]AnoxKaldnes AB, Klosterängsvägen 11A, SE-226 47 Lund, Sweden

Correspondence to: B. Laycock (E-mail: b.laycock@uq.edu.au).

ABSTRACT: This study represents the first detailed analysis of the thermal, morphological, and crystallization properties of the blend components within a range of mixed-culture polyhydroxyalkanoates (PHAs), with 3-hydroxyvalerate content in the as-produced materials and in the fractions ranging from low (12 mol %) to high (91 mol %). Both coarse and fine fractionation of the as-produced copolymers confirmed that they were blends of nominally blocky and/or random copolymers of poly(3-hydroxybutyrate-*co*-3-hydroxyvalerate), with very broad compositional distributions as governed by the PHA accumulation strategy. The crystallization kinetics and thermal properties of the fractions were found to be very significantly different from each other, consistent with the hypothesis that the overall mechanical properties were primarily controlled by the more rapidly crystallizing components. Two materials produced using an alternating feeding strategy demonstrated unique crystallization and thermal properties in their fractions, which are considered to have contributed to distinctly more elastic mechanical properties in these particular samples. © 2014 Wiley Periodicals, Inc. J. Appl. Polym. Sci. **2014**, *131*, 40836.

KEYWORDS: biopolymers and renewable polymers; crystallization; properties and characterization

Received 6 February 2014; accepted 7 April 2014
DOI: 10.1002/app.40836

INTRODUCTION

Microbially produced polyhydroxyalkanoates (PHAs) are thermoplastic polyesters that act as a carbon/energy store for more than 300 species of Gram-positive and Gram-negative bacteria as well as archaea. Recently, these fully biodegradable biopolyesters have attracted much attention as alternative polymeric materials that can be produced from renewable resources. The properties of these biopolymers are affected by the same fundamental principles as those of fossil-fuel–derived polyolefins: a broad range of compositions is available based on the incorporation of different monomers into the PHA polymer structure, with this broad range tailoring subsequent thermal and mechanical properties. They possess mechanical properties that are in some part comparable with those of conventional thermoplastics such as polypropylene and polyethylene. However, brittleness (particularly for poly-3-hydroxybutyrate [PHB]), embrittlement with aging due to secondary crystallization, a relatively narrow processing window, and limited thermal stability are reported as disadvantages.[1] The addition of comonomers such as hydroxyvalerate to the polymer composition is known to reduce melting temperature, increase flexibility, and slightly reduce crystallinity, making the poly(3-hydroxybutyrate-*co*-3-hydroxyvalerate) (PHBV) copolymers attractive alternative materials.[2] Through appropriate processing modifications and the use of additives and/or blends, bioplastics based on compounds with PHB and other PHA copolymers are being used in commercial application today.

The use of mixed cultures for the production of PHA is emerging as a technology to produce environmentally sustainable, lower-cost PHA of varying composition,[3] including PHBV copolymers of high 3-hydroxyvalerate (3HV) content.[4] This biotechnology has a number of advantages, including (i) no sterilization requirements, (ii) an adaptive capacity owing to microbial diversity, (iii) a possibility to use mixed substrates,[5,6] and (iv) concurrent water treatment services in environmental protection.[4] Open mixed-culture PHA production methods have been found that can deliver high PHA contents (~90%) in an enriched microbial consortium over a very short time period of around 8 h.[6]

Additional Supporting Information may be found in the online version of this article.

The mechanical properties of mixed-culture PHAs have in general been inferred from their thermal, molecular weight, compositional, and other properties.[7–9] Until recently, the mixed-culture PHA research literature was lacking in direct studies of the material mechanical properties and of the extent to which the accumulation methods could influence the copolymer distribution. In two recent studies,[10,11] PHBV copolymers of high mol % 3HV content (of 40 mol % in the first case[10] and between 34 and 72 mol % in the second[11]) had thermal and mechanical properties that were consistent with random copolymers of these compositions. However, in other recent work,[2,12] in which a range of feeding strategies was adopted to manipulate the composition and microstructure of poly-3-hydroxybutyrate-*co*-3-hydroxyvalerate (PHBV) copolymers from mixed cultures, it was found that the materials as produced were complex blends. In these blends, one component was consistently found to be a very low 3HV content copolymer, with the other components having much higher 3HV contents. Preliminary fractionation studies using solvent/nonsolvent mixtures of chloroform/*n*-hexane provided further evidence that mixed cultures could produce PHBV blends of broad compositional distribution.[12] Even PHA copolymers from pure cultures have been shown to be blends of broad compositional distribution[13,14] by fractionation. This raises the question of the intercellular and intracellular nature of the blends we have observed for mixed cultures. Metabolic flux analysis does suggest that populations of species in mixed cultures will tend to accumulate different types of copolymers due to differences in substrate preferences.[15]

It is known that the crystallization rate of PHB is orders of magnitude faster than PHBV of ~50 mol % 3HV content,[16] indicating that the nature of these blends could strongly influence the microstructure in cooling from the melt. It is also well known that the physical and mechanical properties of semicrystalline polymers are very dependent on their crystal structures and thermal history. In this work, the interaction between microstructures and material function is examined. More specifically, this is the first detailed attempt to understand how the behavior of components in a PHA blend determines the physical properties of the bulk material. It was demonstrated that the presence of blend components of differing 3HV contents had a very significant effect on overall polymer crystallization rates and crystalline morphology. In addition, it was found that the nominally block copolymeric materials had components in the blend mix that could not be finely fractionated into high- and low-melting components and that many of the fractions that were produced crystallized more rapidly than the as-produced material, despite the presence of both high- and low-melting phases in the differential scanning calorimetry (DSC) thermograms. Such new knowledge about the nature of the copolymer fractions could be exploited in the future to manipulate the final material properties of polymer blends.

EXPERIMENTAL

Recovered mixed-culture PHBV samples were fractionated into fractions of differing composition and/or molecular weight using solvent/nonsolvent fractionation in chloroform/*n*-hexane. The properties and in particular the crystallization rates of the disparate copolymers in the blend were then analyzed to determine the likely impact of compositional distribution on the blend microstructure and hence ultimately on the material mechanical properties.

Materials

Acetic and propionic acids were of >99% purity and were obtained from Merck. Chloroform was of HPLC grade (99.9% purity) and was obtained from Sigma Aldrich. Deuterochloroform ($CDCl_3$) was of high purity and was 99.8 atom % D (Sigma Aldrich). All other chemicals were of at least 98% purity and were obtained from Sigma Aldrich.

Samples

The full details of polymer production and characterization are reported in previous publications.[2,12] In brief, PHBV was accumulated in an activated-sludge Aerobic Dynamic Feeding (ADF) pilot plant operated at AnoxKaldnes (Lund, Sweden) using 100-L batches of mixed liquor with biomass harvested from an ADF enrichment reactor. The accumulation process was controlled to ensure an in-biomass PHBV of high molecular weight according to methods described in WO2011/070544A2.[17] The carbon substrate for the biomass production in the enrichment reactor was fermented whey permeate waste. PHBV was accumulated in the harvested biomass using acetic and propionic acids (HAc and HPr) as the carbon sources, with these acids being fed either as a mixture or sequentially as described below. The fed substrate concentration was always 50 g COD L^{-1}. The polymer was extracted using butanol or acetone subsequent to conditioning the polymer in the biomass to exhibit a high thermal stability.[18] Some molecular weight loss occurs during the extraction process. Purity was determined to be 95–98% for all samples by thermogravimetric analysis using a Q500 thermogravimetric analyzer from TA Instruments. This extracted PHBV was the "as-produced" copolymer used for the material property assessments.

Three different feeding strategies were used to vary the copolymer sequence distribution. The first strategy was to feed the biomass the same mixture of acetic and propionic acids in pulses over the whole accumulation period, in theory producing simple random copolymers with composition dependent on the proportion of acids in the mix.[19] In the second strategy, one type of feed was fed in pulses for a period of 4 h and then a different feed was used for the remainder of the time. This approach was expected to produce some nominally diblock (A–B) copolymer blended with random copolymer, where A–B are segments of homopolymer blocks. The final approach used an alternating feeding strategy, where pulses of acetic and then propionic acid were in turn fed to the biomass throughout the accumulation, with different overall proportions of acetic and propionic acids and different volumes of feed per pulse. This approach was designed to produce nominally repeating multiblock $(A–B)_n$ copolymers. These approaches are grouped into the A, B, and C series, respectively, in Table I, which gives a summary of the properties for the selected recovered biopolymers to be investigated. Sample C6 (Table I) is a previously unreported material that was produced in the same fashion as Sample C1 using alternating feeding of acetic and propionic

Table I. Properties of Polymers as Obtained

Experiment	Feeding sequence (relative percent as g COD)	PHA type anticipated	HV (mol %)	*D*	*R*
A1	HAc : HPr combined 50 : 50 (11.95 h)	Random copolymer	62%	2.3	0.95
A2	HAc : HPr combined 50 : 50 (8 h)		72%	2.6	0.96
A3	HAc : HPr combined 70 : 30 (8 h)		46%	3.0	0.80
A4	HAc : HPr combined 70 : 30 (8 h)		52%	2.6	0.90
A5	HAc : HPr combined 50 : 50 (8 h)		69%	2.9	0.54
B1	HAc : HPr 70 : 30 (4 h) then HAc : HPr 30 : 70 (4 h)	A–B diblocks blended with random copolymer	65%	2.9	0.80
B2	HAc : HPr 30 : 70 (4 h) then HAc : HPr 70 : 30 (4 h)		64%	5.6	0.59
B3	HAc (4 h) then HPr (4 h)		12%	63.1	0.40
C1	HAc (1.0 h) alternating HPr (0.5 h)—8 h total	$(A–B)_n$ repeating multiblocks (including diblocks and triblocks)	43%	19.3	0.44
C6	HAc (0.5 h) alternating HPr (0.5 h)—8 h total		49%	4.5	0.63

acids with 20.5 g COD acetic or propionic acid per pulse, which equated to ~30 min total time for consumption of acid per pulse.

Analytical Methods

PHA monomeric composition (3HB and 3HV) was determined using the gas chromatography method described in the study of Arcos-Hernandez et al.[19] using a Perkin-Elmer gas chromatograph. Calibration was based on reference standards of a biologically sourced PHBV copolymer (30 mol % 3HV; Sigma Chemicals). The calibration standards were prepared using the same method.

SEC analyses were performed using a Waters 1515 HPLC solvent delivery system combined with a Wisp 717 autoinjector, a column set consisting of a Waters Styragel guard column (20 μm, 4.6 mm × 30 mm), and a set of linear columns in series (Waters Styragel HR5: 5.5 μm, 7.8 mm × 300 mm; Waters Styragel HR1: 5 μm, 7.8 mm × 300 mm; and Waters Styragel HR4: 4.5 μm, 4.6 mm × 300 mm) and kept at 35°C with a refractometer/UV–vis detector set at 37°C on elution with chloroform (1 mL/min). The polymer molar mass was calibrated with reference to polystyrene standards. Weight– and number–average molar masses (M_w and M_n) and polydispersity were calculated using the software Breeze 3.30 from Waters.

Quantitative ^{1}H-NMR and ^{13}C-NMR spectra were acquired at 298 K in $CDCl_3$ (10 mg/mL for ^{1}H-NMR and 40 mg/mL for ^{13}C-NMR) on a Bruker Avance 500 spectrometer. The relative peak intensities of ^{1}H-NMR and ^{13}C-NMR spectra were determined using PeakFit Software. T_1 relaxation times were determined using the inversion-recovery method reported previously,[20] and pulses of 45° were used. Chemical shifts were referenced to the residual proton peak of $CDCl_3$ at 7.26 ppm and to the carbon peak of $CDCl_3$ at 77 ppm.

The *D* and *R* values were calculated, where the *D* value represents the extent of the deviation of the copolymer composition from the statistically random composition distribution, and the parameter *R* is the ratio of the number–average lengths of 3HV blocks, L_V^R, to the experimental number–average sequence lengths of 3HV units (L_V^E).[21] These calculations are based on the relative peak intensities of the 3HV-centered diads (in the carbonyl region) and the 3HV-centered triads (for the main-chain and side-chain methylene groups [eqs. (1–5)]:

$$D = \frac{F_{VV}F_{BB}}{F_{VB}F_{BV}}, \tag{1}$$

$$R = L_B^R/L_B^E = L_V^R/L_V^E, \tag{2}$$

$$L_V^R = (k+1)/k, \tag{3}$$

$$L_V^E = (F_{VVV}+F_{VVB}+F_{BVV}+F_{BVB})/(F_{BVB}+F_{VVB}), \tag{4}$$

$$k = [3HB]/[3HV], \tag{5}$$

where *V* and *B* represent 3-hydroxybutyrate and 3-hydroxyvalerate groups, respectively, F_{XY} represents the mole fraction of the *XY* sequence, F_{XVY} represents the mole fraction of the *XVY* sequence, and [3HB] and [3HV] represent the mole fraction of the 3-hydroxybutyrate and 3-hydroxyvalerate groups, respectively.

Attenuated total reflection (ATR)–FTIR spectra were recorded on a Thermo Electron Nicolet 6700 spectrometer equipped with a single-bounce diamond ATR cell. For each sample, three different portions were tested, taking three replicates for each portion. An automatic baseline correction algorithm was used in all spectra to avoid errors due to baseline shifts. Normalization to the sum of the absolute value of all variables included between the bands amide band I (1650 cm^{-1}) and amide band II (1540 cm^{-1}) was performed using 1-Norm algorithm from the software PLS Toolbox® V.5.2.2 (Eigenvector Research). These bands have been assumed to be independent of PHA, and this method has also been shown to account for some of the variation due to changes in sample thickness.[22]

Thermal properties of the polymers were investigated using DSC (TA DSC-Q2000). All runs were performed on 2.0–4.0 mg

Table II. Summary of Fractionations Undertaken in This Study

Bulk material	Fractions
Coarse fractionation	
A1 to A4	$A1_{1-3}$; $A2_{1-3}$; $A3_{1-3}$; $A4_{1-3}$
B1 to B3	$B1_{1-3}$; $B2_{1-3}$; $B3_{1-2}$
C1	$C1_{1-4}$
Fine fractionation	
A1	$A1f_{1-F8}$
A5	$A5f_{1-F7}$
C1	$C1f_{1-F7}$
C6	$C6f_{1-F11}$

samples in a nitrogen atmosphere. The data obtained were used to calculate the glass transition temperature (T_g), crystallization temperature (T_c), cold crystallization temperature (T_{cc}), melting point (T_m), and fusion enthalpies (ΔH_f).

Standard DSC heating and cooling scans were performed at 10°C min^{-1}. No thermal pretreatment was applied in this case. Samples were heated at 10°C min^{-1} to 185°C and kept isothermal for 0.1 min, and then cooled at 10°C min^{-1} to −70°C and kept isothermal for 5 min. After this, the sample was once again heated at 10°C min^{-1} to 185°C, followed by rapid cooling at 100°C min^{-1} to −70°C before being kept isothermal for 3 min. In a final heating ramp, the sample was heated at 10°C min^{-1} to 200°C. The T_m and enthalpy of fusion, ΔH_m, were determined from the first heating ramp. The T_c and ΔH_c were determined from the cooling cycle following the first heating ramp. The T_g and T_{cc} were determined from the final heating cycle. Selected samples were also tested using two other heating rates of 5°C min^{-1} and 20°C min^{-1} to 185°C in a single heating cycle to further examine the origin of multiple melting peaks.

Isothermal crystallization kinetics were evaluated by equilibration of sample at 25°C and then heating at 10°C min^{-1} to 190°C, holding at this temperature for 2 min to remove residual crystals, and then rapid cooling at a rate of ~50°C min^{-1} (the maximum possible) to the predetermined crystallization temperature. After crystallization was complete (as judged by the evolution of the crystallization endotherm), the sample was heated at 10°C min^{-1} to 185°C. For Avrami analysis, samples were only analyzed if the crystallization exotherm commenced after reaching isothermal crystallization temperature, which meant that some samples were excluded due to being partially crystallized at time 0.

The mechanical properties of Sample C6 were determined for solvent cast films using the same method as described previously ($n = 10$).[2]

Isothermal Spherulite Growth Behavior

The spherulitic morphology and crystal growth of the as-produced PHBV copolymers were investigated using two different sets of equipment. One set comprised a polarized optical microscope (Olympus BX50) equipped with a Linkam hot-melt stage (TMS93) and Infinity2 Digital camera. The other comprised an OXJP304 Polarizing microscope equipped with a 3.2 Mpixel ODCM310 Digital camera with an OZ9-TCS temperature-controlled microscope stage and separate hot plate.

In both cases, samples were cast as 5 wt % solutions in chloroform onto a glass coverslip, filtered using a 0.45 μm filter, and then sealed after film formation under another glass coverslips. The samples were then heated to 190°C and then held for 2 min to ensure complete melting, followed by rapid quenching to the crystallization temperature. The spherulitic growth rate (G) was calculated from the change of radius (R) with time (t).

Copolymer Blend Fractionation

The as-produced bacterial PHBV samples were comonomer-unit compositionally fractionated with a chloroform/*n*-hexane mixed solvent at ambient temperature (Table II). Crude, coarse fractionation was carried out to identify the major blend components as a function of feeding strategy. Fine fractionation of selected materials was carried out in attempt to identify and study specific copolymers within the bulk material.

The fractionation procedure for the coarse fractionation was as follows: 2.0 g of original sample was dissolved in 200 mL chloroform, and 1 mL aliquots of *n*-hexane were added slowly to the solution with gentle agitation. On the first sign of cloudiness or any form of sample deposition, the mixture was allowed to stand for 24 h at ambient temperature. The precipitate was then separated from solution by centrifugation (at 3500 rpm for 5 min). The supernatant was decanted and the gradual *n*-hexane addition followed by centrifugation procedure was repeated until further addition did not yield any more precipitate. The hexane content in the solvent/nonsolvent mixture at the precipitation point for each material fraction is given in Table I. All of the recovered polymers were dried in a vacuum oven at 60°C for 24 h and stored at 25°C and 50% relative humidity for 2 weeks before use.

The fine fractionation technique was essentially the same, with the exception that a larger additional mass of polymer was dissolved in chloroform (with 20.9 g polymer A2 in 780 mL chloroform, 22.1 g polymer C1 in 900 mL chloroform, and 4.1 g polymer C6 in 300 mL chloroform as starting solutions), and much more time (at least 10 min) was allowed after the addition of each 10 mL aliquot of *n*-hexane before further aliquots were added.

RESULTS

Coarse Fractionation of As-Produced Copolymer Blends

The objective of these studies was to examine the extent to which feeding strategies could be used for manipulating microstructures of mixed-culture PHBV. It was found[2] that it was possible to produce polymers that were apparently more random or blocky in nature. However, given that it is well known that as-produced PHBVs from both pure and mixed cultures have a broad comonomer unit compositional distribution,[13,23–25] this conclusion was complicated by the presence of blends in the as-produced materials. It was necessary to isolate fractions of these blended materials to properly characterize the properties of random or blocky PHBVs.

There are a number of methods for characterizing the blend composition of a bulk polymer sample, such as gradient

polymer elution chromatography.[26] However, solvent/nonsolvent fractionation is a well-established technique that has been used successfully to characterize the compositional distributions in both pure and mixed cultures.[13] The results of the solvent/nonsolvent fractionation for selected mixed-culture PHBV samples extracted from PHA-rich biomass, contrasting the properties of the initial polymer blend with the recovered blend fractions, are summarized in Table III. These initial solvent/nonsolvent fractionation results, even though quite coarse and leading to between two and four fractions at most (Table III), show quite clearly that the compositional distributions for the as-produced copolymeric materials is very broad, in line with previous results.[12] The differences in 3HV content between fractions of a single material were as high as 57 mol % (for Sample A1), with the smallest difference being 33 mol % (for Sample A4).

Molar masses (M_w and M_n) for the fractions derived from the samples were in general lower than for the as-produced materials and also for some samples showed some decrease with each successive fraction.

This is in contrast to expectation[13,14,27,28] and, particularly given the fact that the first fraction shows a drop in comparison with the starting material, may reflect either some degradation and/or influence of chain length on separation. However, the respective 3HV contents for the fractions did correlate roughly with percent hexane, suggesting that fractionation was primarily caused by the type and morphology of the respective polymers in the blend. There was in general little change in the polydispersity.

NMR Analysis of Blends and Blend Fractions

Having successfully isolated fractions of very different compositions, we considered in further detail the comonomer sequence distributions in the fractions using the methods proposed by Kamiya et al.[29] and Žagar et al.[21] The D and R values were calculated, where the D value represents the extent of the deviation of the copolymer composition from the statistically random composition distribution, and the parameter R is the ratio of the number–average lengths of 3HV blocks, L_V^R, to the experimental number–average sequence lengths of 3HV units (L_V^E)[21] (see "Experimental Section" for details of calculations). A sample with $D > 1.5$ is regarded as being either a mixture of two or more random copolymers or a blocky copolymer,[29] and if $D > 5$ or so, the sample is either a biphasic or multiphasic blend or a blocky copolymer. D is not sensitive to the broad chemical compositional distribution of PHAs.[30] The parameter R gives more sensitive information on chemical composition distribution[21] and has a value of 1 for a completely random distribution of 3HB and 3HV units in the copolymer chain and 0 for a diblock copolymer.

The relative intensities of the experimentally determined diad and triad sequences were also compared experimentally with three models, these predicting outcomes for a completely random distribution of 3HB and 3HV monomer units (Model 1, estimated using Bernoullian statistics), for block copolymeric distribution estimated using a first-order Markovian model (Model 2), and for a mixture model predicting the outcome for a mixture of two random copolymers, again using Bernoullian statistics (Model 3). The methodology adopted here is detailed in the studies by Kamiya et al.[29] and Wei et al.[11] The diad and triad sequence data, the D and R values, and the data theoretically estimated using the random, blend, and block statistical models are given for selected blend fractions in Supporting Information Table S1. In this table, A, B, and X represent the best fit for a mixture model, where A is the mol % 3HV content of the first copolymer in the blend, B is the mol % 3HV content of the second copolymer, and X represents the proportion of A in the blend. F_V and F_B represent the mole fraction of the 3HV or 3HB groups, respectively, and SSE is the sum of squared errors of prediction between the model fit and the experimental data.

For the samples with D and R values near 1, the observed sequence distributions were in general compatible with model 1 (a simple random copolymeric structure). This includes samples A2 Fractions 1, 2, and 3, and A4 Fractions 2 and 3. This is consistent with the results obtained by Wei et al.[11] who also studied mixed-culture PHBVs of high HV content and found that a good fit to a Benoullian model of random monomer unit distribution was obtained for their materials. In that study, electrospray ionization-mass spectrometry of the oligomers obtained after partial alkaline hydrolysis also demonstrated random monomer unit distribution in the copolymers obtained.

The remaining samples exhibit D and R values well away from 1 and are a very poor fit to the random copolymer model 1. However, the distinction between Models 2 and 3 (block copolymers or mixtures) is not easy, as the fit is not ideal for either. For A4 Fraction 1, for example, Model 2 (block copolymer) has the lowest SSE; this model, however, is also not an optimal fit based on the fact that the SSE is still high, indicating that the material is more complex than any of these simple models would indicate. B2 Fraction 2 also does not fit well to any model, although a blend gives the best fit of the three in this case. Likewise, B2 Fraction 1 and B3 Fraction 1 could be blends of PHB and a random copolymer but could also be more complex structures/mixtures, whereas C1 Fractions 1 and 2 and B3 Fraction 2 appear to be a blend of polyhydroxyvalerate and a random copolymer.

Overall, the D and R values and the model fits are good for distinguishing true random copolymers of relatively narrow compositional distribution from blends or block copolymers, but are not adequate for distinguishing between block copolymers and blends, particularly where, in this case, we probably still have blends and/or blocks present in mixtures even in the fractions.

Thermal Properties of Fractions

We have been working toward establishing structure–function relationships by seeing how manipulation of accumulation strategies could influence copolymer morphologies, which in turn would govern microstructure and resulting mechanical properties. Given that microstructures are influenced by the material crystallization during melt processing, the presence of blends is likely to have a significant impact. It was therefore important to consider how the crystallization behavior of the respective fractions could influence the formation of microstructures for the

Table III. Properties of Fractions of Solvent/Nonsolvent Fractionated Mixed-Culture PHBV

Sample	Fraction	Hexane in solvent (vol %)	% Mass fraction	HV (mol %) by gas chromatography[a]	M_n (g mol^{-1} × 10^5)	M_w (g mol^{-1} × 10^5)	PDI	T_g (°C)	T_m (°C) Under 110°C	ΔH_m (J g^{-1})	T_m (°C) Over 110°C	ΔH_m (J g^{-1})	ΔH_m (J g^{-1}) Total
A1	As-produced		100	62%	2.6	4.6	1.9	−12.8/0.1	80.6/94.9	33.3	143.1/156.6	2.5	35.8
	1	66	11	26%	1.5	3.4	2.3	−11.3/1.3	84.5	2	135.1/153.7	43	45
	2	70	17	50%	1.5	3.1	2.0	−6.0	73.2	25.3	154.1	5.2	30.5
	3	80	72	80%	1.3	2.7	2.1	−11.8	73.5/91.8	64.9	-	0	64.9
	R[b]		83										
A2	As-produced		100	72%	2.3	5.2	2.2	−11.7	71.7/87.5/97.6	60	-	0	60
	1	68	34	57%	1.9	3.9	2.1	−7.1	72.3	35.4	159.5/169.6	2.5	37.9
	2	71	42	75%	1.6	3.5	2.3	−11.8	84.1/95.0	59.2	-	0	59.2
	3	76	24	87%	1.1	2.9	2.7	−13.1	92.9	65.3	-	0	65.3
	R		94										
A3	As-produced		100	46%	2	4.5	2.3	−10.3/−1.2	77.5	19	159.2	13.7	32.7
	1	62	44	38%	1.6	3.5	2.2	−7.2/1.7	73.4	14.5	137.9/159.1	27.1	41.6
	2	71	55	59%	1.4	2.9	2.1	−7.6	75.5/91.9	41.4	122.8/134.8	2.9	44.3
	3	82	1	74%	n.d.	n.d.	n.d.	−12.5	88.5/97.6	50.4	-	0	50.4
	R		94										
A4	As-produced		100	52%	2	4.6	2.3	−10.5/0.5	80.3/91.7	20.4	156.3	9.3	29.7
	1	66	42	40%	1.7	3.8	2.3	−9.5/1.0	75.9	6.8	132.3/154.4	29.4	36.2
	2	73	42	63%	1.5	3.3	2.1	−6.7	71.7	32.4	154.5	0.3	32.7
	3	79	16	77%	1.3	2.9	2.3	−11.3	81.1/91.7	40.8	-	0	40.8
	R		95										
B1	As-produced		100	65%	2.5	5.5	2.2	−14.3/1.0	85.0/98.4	32.7	154.8	7.4	40.1
	1	66	18	45%	1.9	4.2	2.2	−13.6/ −4.7/0.0	69.9/85.2	19.3	136.6/154.0	13.4	32.7
	2	69	21	51%	2.1	4.3	2.1	−7.7	65	21.4	-	0	21.4
	3	74	61	91%	1.6	3.8	2.3	−14.6	73.1/94.0	61.1	-	0	61.1
	R		94										
B2	As-produced		100	64%	2.2	5.1	2.3	−15.1/0.5	85.0/98.3	35.5	154.7	6.9	42.4
	1	64	33	39%	1.9	4.3	2.3	−13.0/3.4	69.0/91.5	13	136.4/154.4	33.1	46.1
	2	73	29	81%	1.8	3.8	2.1	n.d.	69.4/87.8/99.4	45.7	-	0	45.7
	3	77	38	91%	1.9	4.1	2.2	−14.2	95	71.9	-	0	71.9
	R		91										
B3	As-produced		100	12%	2	4.5	2.3	1.8	80.3/92.2	2.1	169.5	61.3	63.4
	1	41	94	12%	1.5	3.4	2.3	4.7	78.3	2.7	144.9/172.1	84.2	86.9
	2	84	6	67%	1.9	4.5	4.2	−10.7	68.5/84.9	36	137.5	2.5	38.5

Table III. *Continued*

Sample	Fraction	Hexane in solvent (vol %)	% Mass fraction	HV (mol %) by gas chromatography[a]	M_n (g mol^{-1} × 10^5)	M_w (g mol^{-1} × 10^5)	PDI	T_g (°C)	T_m (°C) *Under 110°C*	ΔH_m (J g^{-1})	T_m (°C) *Over 110°C*	ΔH_m (J g^{-1})	ΔH_m (J g^{-1}) Total
	R		82										
C1	As-produced		100	43%	2.1	4.6	2.2	−13.2/1.5	84.3/98.7	17.6	169.2	25	42.6
	1	50	68	35%	1.7	3.8	2.2	−13.0/3.4	86.5	18.2	141.3/166.0	44.9	63.1
	2	65	29	61%	1.6	3.4	2.1	−12.2	76.9/91.8	35.5	165	12.6	48.1
	3	81	1	80%	1.4	3.2	2.3	−15.7	96.0/102.5	35.7	156.8/170.1	1.3	37
	4	93	2	79%	1.1	3.8	3.3	−12.9	86.1/93.5/103.5	57	165.9	1.1	58.1
	R		98										

[a] Composition as determined by ^{1}H-NMR matched very closely with these results and hence values are not shown.
[b] R in this table represents total recovery of polymer from initial mass.

as-produced materials. The thermal and crystallization properties of the as-produced and fractionated samples were investigated using DSC.

The first DSC heating scans are given in Figure 1. It should be noted that if the second heating scan was selected, the peaks of lower T_m values would not be present as these require a long time (days) to crystallize. Most of the coarse fractions exhibited simpler melting behaviors than the original as-produced material, as characterized by fewer and sharper melting peaks.

It is well known that blends of PHBV copolymers of differing 3HV content vary from complete miscibility through to complete phase separation depending on the relative 3HV content of the different components, with phase separation typically occurring if the difference in 3HV content is at least 15 mol %.[14] It is also known that apart from the presence of different copolymers in a blend, multiple melting peaks can be attributed to (i) melting, recrystallization, and remelting during heating, (ii) the presence of more than one crystal modification, (iii) different morphologies, (iv) physical aging, (v) different molar mass species, (vi) orientation effects, and so forth.[14] In this case, the multiple melting peaks and T_gs were attributed to both melt-recrystallization and microphase separation in the blends. The microscopy results (see "Crystallization Behavior: Polarized Optical Microscopy" section) also show evidence of microphase separation for some samples. Some of the remaining multiple melting peaks could be attributed to occurrence of melt-recrystallization based on multiple heating scan rates (data not shown). As it was difficult to ascertain in all cases which peaks were due to melt-recrystallization, all melting peaks are therefore reported in Table III and Figure 1.

For those fractions that only had a single T_g, and hence could be presumed to be either a single copolymer or a homogeneous miscible polymer blend, a linear relationship to comonomer content was generally observed as has been previously reported (Figure 2).[28] When multiple T_gs were present, there was no relationship with overall composition, indicating the presence even in the coarse fractions of microphase-separated blends or block copolymers.

For the as-produced materials,[12] the melting temperatures could be clustered into low-melting (<100°C) and high-melting (>130°C) temperature components (Figure 2). On fractionation, the nominally random copolymeric materials (A1–A4) were generally observed to divide into fractions that discriminated between the low- and high-melting temperature components. The first fraction was usually rich in a very low 3HV content copolymer (with melting points close to pure PHB), whereas the other fractions all had higher 3HV contents and low melting temperatures. Sample A2 (at a high 72 mol % 3HV content overall) was the only polymer that did not have a low 3HV content (high melting) component present in its fractions. The NMR results given in the "NMR Analysis of Blends and Blend Fractions" section suggest that the fractions of these Group A (random copolymeric) samples were all random copolymers or copolymer blends. Therefore, the biomass used for the current study tended to produce a blend of PHBV random copolymers over a range of 3HV contents when fed a

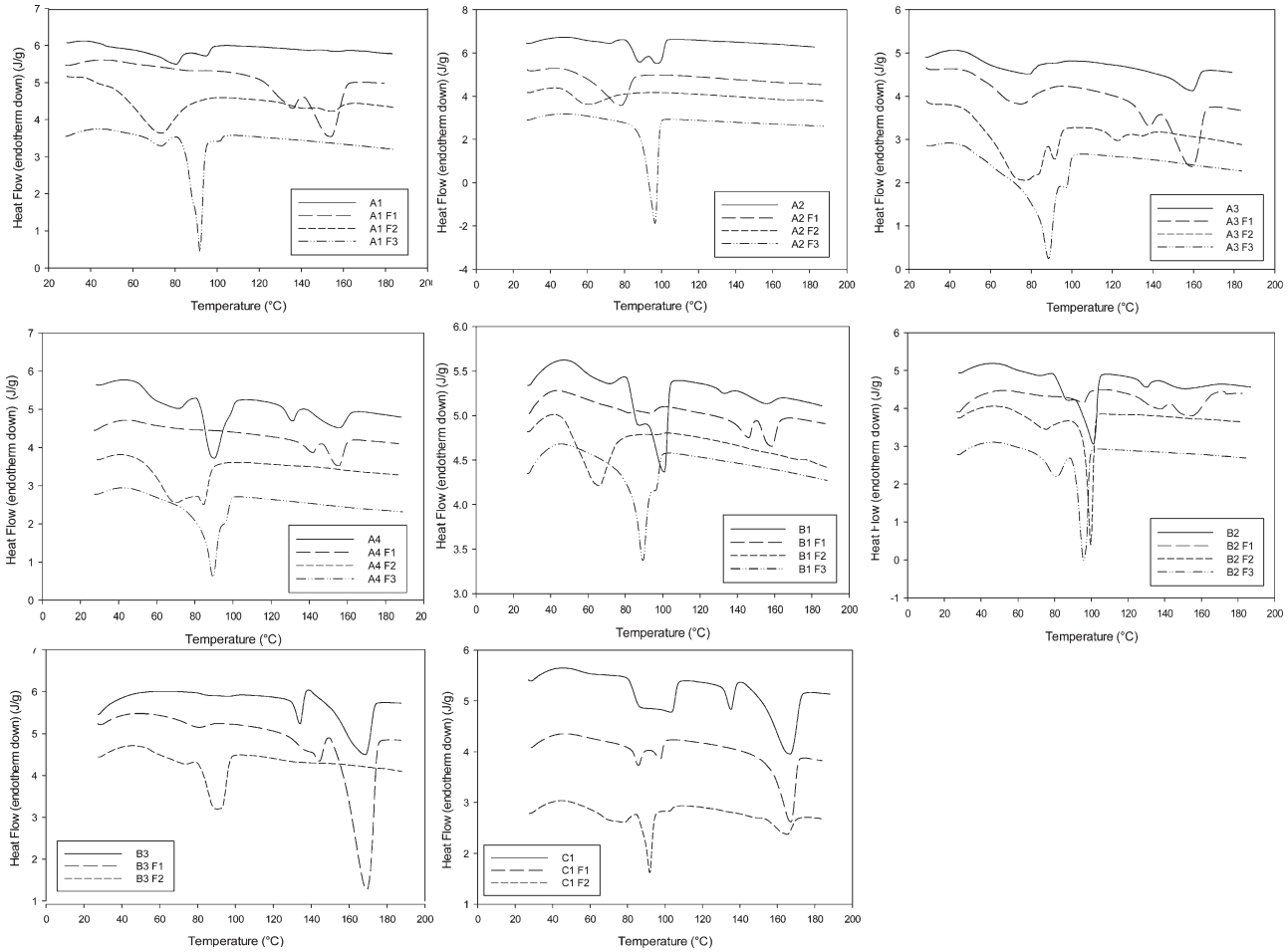

Figure 1. DSC thermograms showing melt transitions during the first heating scan for as-produced PHBV copolymers and their fractions.

substrate mixture of acetic and propionic acids. This biomass was originally enriched on a fermented whey permeate, which was dominated by butyric and acetic acids and low in propionic acid (with the acid mix comprising 43% acetic, 1.6% propionic, 0.2% isobutyric, 50.3% butyric, 1.7% valeric, and 2.6% caproic acids). Such a mixture when used for PHA accumulation tends to produce a PHBV copolymer with only a few mol % 3HV content. It has been demonstrated by Lemos et al.[31] that the response of biomass to different feedstocks varies depending on the substrates to which that biomass is adapted. In this case, it is probable that within the enriched biomass population, there are some organisms that are able to use acetic acid only, producing PHB, or to use only some propionate to produce a low 3HV content copolymer, and other organisms that are capable of utilizing the propionic acid to produce higher 3HV content copolymers.

The B group samples were nominally A–B diblocks blended with random copolymers. However, the results (Figure 1) were very similar to those for Samples A3 and A4 (which were most likely blends of random copolymers). Again there was a range of 3HV contents, with the first coarse fraction typically having high to very high *D* values (higher than those for the A group samples). For this first coarse fraction, both high- and low-melting peaks were present, with two T_gs typical of high and low 3HV content copolymer, indicative of a phase-separated blend or a block copolymer or a mix of both. The second and third fractions of the B group samples were characteristic of random copolymers and very similar to the random copolymeric fractions from the A group, with very little high-melting temperature component present. The *D* and *R* values for these fractions reflect this, with likely still some blends present but unlikely to be block copolymers. These samples were prepared by running the accumulation for 4 h using one reagent type (either pure acetic acid or mixed acetic and propionic acids) and then switching to another. It would only be the proportion of chains that were growing at the time of the transition and that were in organisms that were capable of incorporating both reagent types into the growing polymer chain and that also had the enzymes capable of doing so that would be able to produce block materials. Based on the results presented here, the proportion of block copolymers is likely to be at most a very small fraction of the polymer present.

By contrast, Sample C1 (the nominally blocky material) retained both high- and low-melting components in both fractions. To

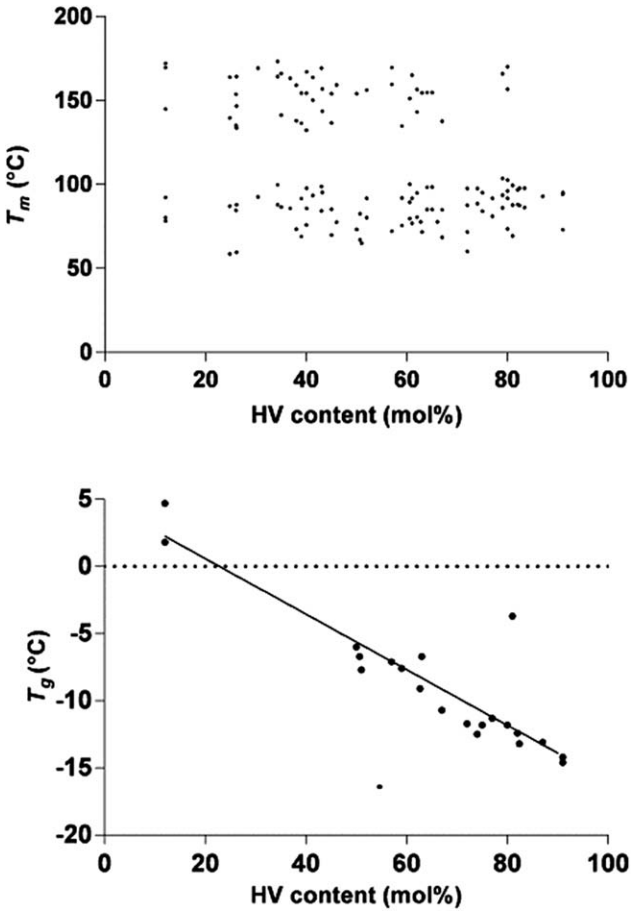

Figure 2. Graph of melting temperatures (top) for all PHBV samples (as-produced and fractionated) and glass transition temperatures (bottom) for samples with a single T_g, as a function of HV content.

test if these two distinct T_m components could be separated under more careful fractionation conditions, four samples (two random copolymer blend materials A2 and A5 and the two nominal block copolymers C1 and C6) were finely fractionated.

Fine Fractionation

The results of the fine fractionations are given in Table IV and Figures 3–5. The number of fractions produced ranged between 7 and 11, which is far more detailed than for the coarse fractionations.

For the random copolymer A2, there was very little material present of less than 51 mol % 3HV content, with the first three fractions (ranging from 24.8 to 36.8 mol % 3HV) representing only 2.7% of the mass. These were the only fractions that had any high-melting components and were probably still blends. The remaining fractions ranged from 50.7 to 82.4 mol % 3HV and were all clearly random copolymers with single T_gs (pure copolymers or miscible blends). In contrast to the coarser fractions, fine fractionation of this material was based initially on differences in 3HV contents with molar mass (both M_w and M_n) decreasing only slightly as 3HV content increased. There was a significant decrease in molar mass for the last two fractions (10% of the mass), and for the final fraction, there was a decrease in 3HV content as well. This is probably due to the lower molar mass fraction being more soluble despite the lower 3HV content, although Wang et al.[28] have suggested that the increase in crystallizability as 3HV content increases above 50 mol % may be responsible for a reversal of the solubility effect. Thus, the blend separation in the solvent was interpreted to be due to factors other than the respective fraction polymer chain length. For PHBVs, the fractionation is presumed to be due to the distinctive polarities of the different pendant chains at the β-site.[21]

The other random copolymer A5 gave similar results to A2, in that only 12% of the material contained any significant high-melting (low 3HV) content copolymer and the rest was cleanly fractionated into copolymers with single glass transition temperature. There was a regular decrease in T_g, and T_m was in line with expectations based on 3HV content and molar mass. Overall, therefore, the random copolymeric materials made with 50 : 50 acetic and propionic acids on a gCOD basis as a combined feed produced blend copolymers of a broad compositional distribution that could be repeatably fractionated into clean random copolymers of differing 3HV content.

By contrast, both the materials made using alternating feeding of acetic and propionic acids (again at 50 : 50 g COD equivalent) produced materials that in the main could not be fractionated cleanly into high- and low-melting copolymers.

For the nominally block copolymer C1, the first five fractions (which represented 82% of the as-produced material) had high D and low R values, with both high- and low-T_m portions and two T_gs present. The 3HV contents also varied little between fractions, actually decreasing for Fraction 2. It was only for the last two fractions that the 3HV content changed significantly, with little or no high-melting components present. T_ms decreased slightly for the high-melting component for Fractions 4 and 5.

A very similar pattern was observed for the nominally block copolymer C6, with in this case 52% of the material (the first five fractions) having both the high- and low-melting components and two glass transitions indicative of high and low 3HV content domains. These results of fractionation are compatible with the interpretation that a blend of block copolymers of similar 3HV content was generated by the C-accumulation feed strategy and that the blocky nature of the blend components results in distinct differences in solvent solubility as does changes in 3HV content.

Isothermal Crystallization Kinetics: DSC

The kinetics of crystallization play a central role in determining the final mechanical properties of the polymer, and hence a detailed analysis of the isothermal crystallization kinetics for each of the fractions was undertaken to compare with the data reported for the as-produced material.[12] As determination of the absolute degree of crystallinity is not necessary during data treatment in crystallization kinetics, the relative crystallinity as a function of temperature was defined as follows[32]:

$$X_t = \int_0^t (\mathrm{d}H_c/\mathrm{d}t)\mathrm{d}t \Big/ \int_0^\infty (\mathrm{d}H_c/\mathrm{d}t)\mathrm{d}t, \qquad (6)$$

where the first integral is the heat generated after time t, and the second integral is the total heat of crystallization for $t = \infty$.

Table IV. Fine Fractionation of PHBV Samples A2 and A5 (Random Copolymer Blends) and C1 and C6 (Nominally Blocky Copolymers)

Sample	Fraction	Hexane in solvent (vol %)	%Mass fraction	HV (mol %) by gas chromatography	M_n (g mol^{-1} $\times 10^5$)	M_w (g mol^{-1} $\times 10^5$)	PDI	T_g (°C)	T_m (°C) Under 110°C	ΔH_m (J g^{-1})	T_m (°C) Over 110°C	ΔH_m (J g^{-1})	ΔH_m (J g^{-1}) Total	D	R
A2	As-produced		100.0	72	2.3	6.3	2.7	−11.7	71.7/87.5/97.6	60.0	-	0.0	60.0	2.6	0.96
	1	53.6	1.5	37	2.0	5.0	2.4	−11.0/0.2	85.8	22.5	163.2	28.8	51.3	7.5	0.49
	2	57.7	0.3	25	2.2	5.4	2.4	−11.5/−0.5	58.6/87.0	4.4	139.6/163.9	40.1	44.5	10.1	0.58
	3	61.8	0.9	26	2.3	5.2	2.2	−2.3	59.6/87.9	1.9	133.6/146.8/164.2	35.2	37.1	3.0	0.65
	4	64.2	9.5	51	2.5	4.8	2.0	−6.7	67.1/82.6	28.9	-	0.0	28.9	1.2	0.91
	5	67.8	44.6	63	1.9	3.8	2.0	−9.1	77.7	48.8	-	0.0	48.8	1.3	0.94
	6	70.3	34.0	82	1.9	4.1	2.2	−12.4	88.1/96.7	61.3	-	0.0	61.3	1.6	0.91
	7	74.6	8.8	82	1.2	2.5	2.2	−13.2	87.4/97.8	67.4	-	0.0	67.4	1.6	0.81
	8	81.3	0.5	66	0.4	0.6	1.3	−10.4	77.7	57.1	-	0.0	57.1	1.3	0.90
	R		86.0												
A5	As-produced		100.0	68	2.1	4.1	2.0	−11.8/1.4	88.8	49.7	160.6	2.8	52.5	2.9	0.54
	1	63.0	12.8	39	n.d.	n.d.	n.d.	−11.3/0.8	87.8/97.1/102.2	37.8	113.9/130.7/160.6	6.4	44.2	5.1	0.63
	2	67.5	19.4	54	1.4	4.1	2.8	−5.5	73.5/93.2	52.9	162.5	0.2	53.1	1.8	0.77
	3	70.5	32.0	77	1.8	5.6	3.1	−10.1	83.5	50.4	-	0.0	50.4	1.0	0.82
	4	72.5	17.6	83	2.2	7.2	3.2	−12.0	92.4	63.1	-	0.0	63.1	1.6	0.86
	5	73.2	6.6	87	1.0	2.0	2.0	−12.9	93.5	64.0	-	0.0	64.0	1.4	0.98
	6	73.8	6.1	73	0.3	0.8	2.4	−13.0	84.1/97.7	54.4	136.5/165.3	1.3	55.7	1.2	0.91
	7	>74	5.5	74	0.3	0.5	1.8	−15.5	78.2	56.2	141.1	0.2	56.4	1.1	0.83
	R		84.0												
C1	As-produced		100.0	43	2.1	5.9	2.8	−13.2/1.5	84.3/98.7	17.6	169.2	25.0	42.6	19.3	0.44
	1	25.0	2.2	40	1.8	6.3	3.5	−16.1/2.1	85.8/97.7	19.8	167.1	31.2	51.0	13.5	0.51
	2	31.6	21.4	30	1.8	6.3	3.6	−14.2/3.1	92.6	24.2	169.3	39.3	63.5	16.0	0.39
	3	40.9	39.9	34	2.3	8.3	3.6	−11.9/3.5	87.9/99.8	22.5	164.2/173.2	30.0	52.5	22.5	0.43
	4	45.7	15.7	41	2.7	5.5	3.3	−15.4/2.5	93.4	18.2	150.2/163.7	38.1	56.3	14.4	0.43
	5	54.6	2.9	43	2.7	5.3	3.2	−15.2/−2.5	95.2	22.2	143.6/156.9	23.5	45.7	7.1	0.46
	6	66.3	10.9	61	2.0	5.3	2.6	−12.5/−5.4	79.7/89.4/100.1	33.6	151.2	2.3	35.9	3.7	0.58
	7	87.8	7.0	83	1.2	3.8	3.2	−12.3	86.2/97.7	54.8	-	0.0	54.8	1.5	0.72
	R		79.0												
C6	As-produced		100.0	50				−13.4/0.8	84.6/94.7	34.5	141.9/160.1	10.5	45	4.5	0.63
	1	40.0	1.2	47				−12.7/−1.1	89.0/97.5	25.2	164	19.2	44.4	5.4	0.64
	2	50.0	6.3	35				−14.0/0.4	89.7	23.7	152.6/164.8	28.8	52.5	7.2	0.54
	3	61.5	27.7	30				−12.3/−0.3	90.6	19.2	162	20.3	39.5	9.5	0.48
	4	64.8	9.0	30				−12.6/−1.8	61.7/90.5	17.1	133.7/159.1	28.5	45.6	5.7	0.57

Table IV. *Continued*

Sample	Fraction	Hexane in solvent (vol %)	%Mass fraction	HV (mol %) by gas chromatography	M_n (g mol^{-1} × 10^5)	M_w (g mol^{-1} × 10^5)	PDI	T_g (°C)	T_m (°C) Under 110°C	ΔH_m (J g^{-1})	T_m (°C) Over 110°C	ΔH_m (J g^{-1})	ΔH_m (J g^{-1}) Total	D	R
	5	66.4	8.2	31				−11.7/−4.2	89.5/100.2	12.7	157.8	5.2	17.9	4.7	0.73
	6	67.9	5.9	45				−6.6	67.3/88.2	34.8	-	0	34.8	1.4	1.07
	7	69.8	10.4	53				−7.9	79.3	46	-	0	46	1.4	0.95
	8	72.2	8.4	79				−13.7	96.1	74.6	-	0	74.6	1.7	0.93
	9	74.2	13.2	71				−11.4	93.8	70.9	-	0	70.9	1.4	0.83
	10	76.0	7.0	77				−13.9	90.5/98.9	66.1	-	0	66.1	1.6	0.89

[a] *R* in this table represents total recovery of polymer from initial mass.

The crystallization exotherms of the rapidly crystallizing fraction for those samples that have a component that crystallizes rapidly enough at 70°C to be measured (i.e., the fraction melting above 110°C) are given in Figure 6 (where for C1, the coarse fractions are analyzed in this case). It is clear that, for all samples, the first fraction crystallized much faster than the initial as-produced material. For the low 3HV content material B3, the first fraction crystallized too fast at this temperature for an exotherm to be recorded, and for sample B1 (a high 3HV content material), the as-produced blend was too slow to crystallize to be included in this set of results.

The Avrami equation was used to quantify the isothermal crystallization kinetics. It assumes the development of relative crystallinity (X_t) with time (t) and can be described by the following equations:

$$1-X_t = e^{-kt^n}, \tag{7}$$

$$\ln\left[-\ln\left(1-X_t\right)\right] = -\ln k + n\ln t, \tag{8}$$

where n is the Avrami exponent, which depends on the nature of nucleation and growth geometry of the crystals, and k is a rate constant that incorporates both nucleation and growth rate parameters.

The Avrami parameters (n and k) were obtained from the plots of $\ln[-\ln(1-X_t)]$ versus $\ln t$, for values of X_t from 10 to 90%. Only samples where the correlation coefficient r^2 for this plot was >0.99 were included in the final dataset. The values for n and k at the temperature at which the crystallization was fastest for each sample are given in Table V, as is the experimentally determined half-life crystallization time ($t_{1/2}$), defined as the time required to achieve 50% of the final crystallinity, and the calculated $t_{1/2}$, derived from the following equation:

$$t_{1/2} = \left(\frac{\ln 2}{k}\right)^{1/n}. \tag{9}$$

In this Table V, the fractions of C1 tested were from the original coarse fractionation. It should be noted that when there were two phases of crystallization (one that was fastest at ~70–80°C and that was due to the high melting portion and another that was much slower and fastest at ~20–40°C), the kinetics for the fastest crystallizing phase was reported. The average value for the Avrami constant n is 2.1 ± 0.4, in line with previous results and the literature.[1,12,33] Although fairly variable, particularly for the samples that took a very long time to crystallize, these n values indicate that the as-produced polymers and fractions had a similar mechanism of crystallization, despite the blend nature of many of these materials, and are indicative of a two-dimensional, circular, athermal, and diffusion-controlled crystallization process with heterogeneous nucleation. There was a good match between experimental and calculated $t_{1/2}$.

The equilibrium melting point (T_m^0) is one of the important parameters for the analysis of crystallization kinetics, as the difference between this value and the crystallization temperature (the degree of undercooling) strongly influences the crystallization rate and morphology. It is obtained from the Hoffman-Weeks equation as follows:

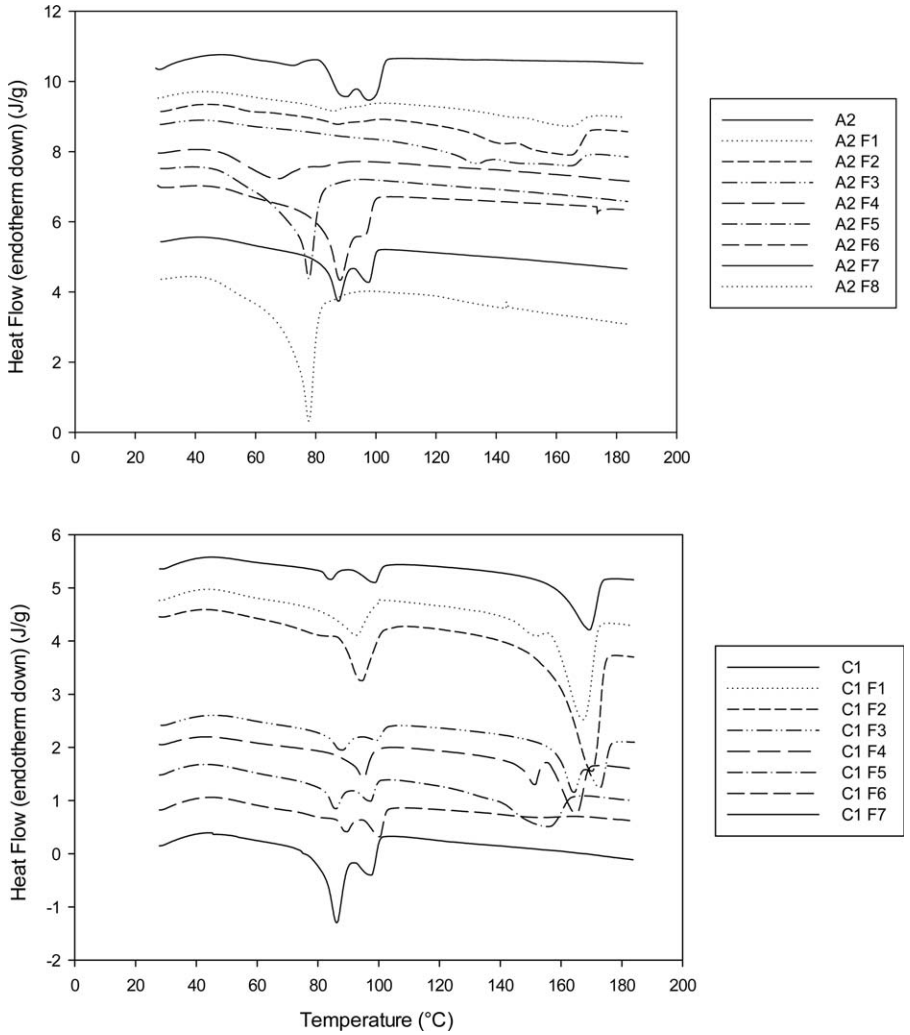

Figure 3. DSC thermograms showing melt transitions during the first heating scan for finely fractionated polymers A2 (top) and C1 (bottom).

$$T_m = T_m^0\left(1-\frac{1}{\gamma}\right)+\frac{T_{iso}}{\gamma}, \quad (10)$$

where γ is the ratio of final to initial lamellar thickness. T_m^0 is obtained by plotting T_m against the isothermal crystallization temperature (T_{iso}) and extrapolating the best line of fit to intersect with the line for $T_m = T_{iso}$. The equilibrium melting temperatures for the high-melting components (and for the low-melting component for B1 Fraction 3) and the nucleation constant of crystal growth kinetics are also given in Table V for those samples where the crystallization was rapid enough to be able to determine these values. The T_m^0 values for the as-produced materials are in general slightly lower than for the first fraction, indicating some depression due to blending, a common phenomenon. The values of T_m^0 for the first fraction range from 171.6 to 180.9°C. In the literature, the T_m^0 for PHB of molar mass >300,000 is around 194 to 197°C,[34,35] with 6 mol % 3HV having a value of 186°C, 12 mol % 3HV being 173°C, and 16 mol % 3HV being 167°C.[34]

The value of $\frac{1}{\gamma}$ lies between 0 (for the most stable crystals where $T_m = T_m^0$ at all crystallization temperatures) and 1 (in the case of inherently unstable crystals). There did not appear to be a consistent trend for the stability of the crystals of the fractions in comparison with the as-produced materials. Some of the materials (such as B1 and B2) had less stable crystals than the others, whereas the low 3HV content B3 and the nominally block copolymer C1 had $\frac{1}{\gamma}$ values comparable with that reported for pure PHB (of 0.1413).[36]

The k values for Sample B1 and its fractions at different temperatures are given in Figure 7. Because there is such a large difference between them, the values have also been plotted on a log scale (Figure 7). The k values for other samples and their respective fractions are also given in Figure 8. A number of consistent trends were observed. Overall, in line with expectations from the literature,[16,37] the different fractions were orders of magnitudes different in crystallization rates. The fractions with 3HV contents around the pseudo-eutectic (which is at around 50 mol % 3HV content[38]) were found to be slowest to crystallize (by orders of magnitude) in comparison with those of lower or higher 3HV content, taking days to complete. The rate of crystallization of the as-produced material was also, in general, considerably slower

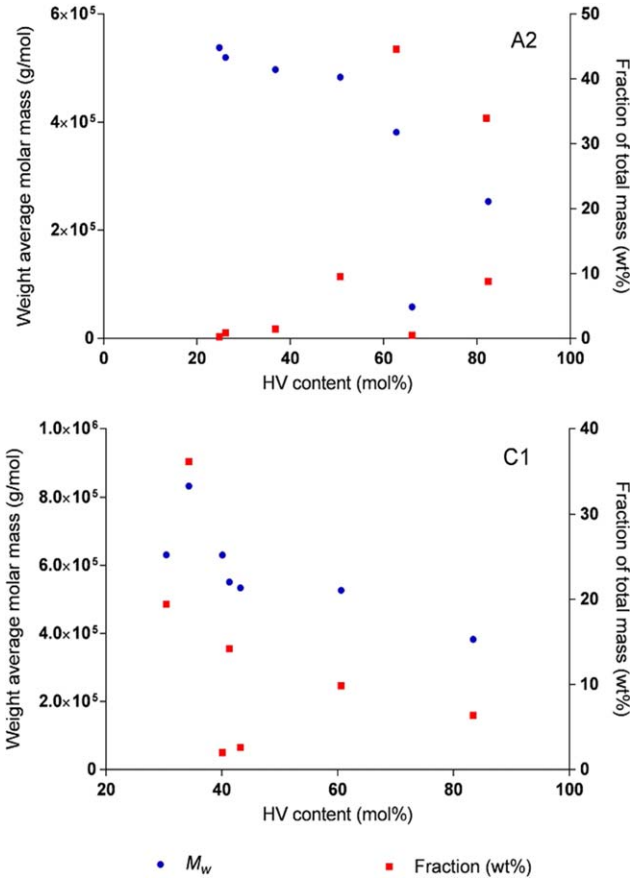

Figure 4. Mass and molar mass distributions relative to 3HV content for the fine fractions of A2 (top) and C1 (bottom). [Color figure can be viewed in the online issue, which is available at wileyonlinelibrary.com.]

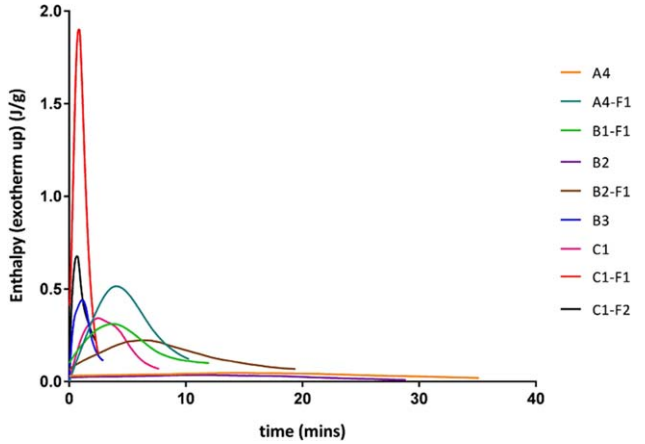

Figure 6. Crystallization exotherms for PHBV copolymers crystallized from the melt at 70°C. [Color figure can be viewed in the online issue, which is available at wileyonlinelibrary.com.]

than that of the lowest 3HV content fraction, indicating that the presence of the other copolymers in the blend acts to hinder the crystallization process. The higher 3HV content fractions (>40 mol % 3HV) also clearly crystallize fastest at a much lower temperature than the low 3HV content components, which were found to reach maximum crystallization rates in the range between 70 and 90°C. In addition, when there were two phases present in the same material (i.e., two T_gs and both high and low melting components present), as observed for the original as-produced material,[12] the lower melting portion crystallized at a much slower rate than the higher melting one. This was the case for the blocky material C1 and its fractions as well (both coarse and finely fractionated).

Crystallization Behavior: Polarized Optical Microscopy

The crystallization of some of the as-produced materials and fractions from the melt state was examined under isothermal conditions at various crystallization temperatures (T_{iso}s) using polarized optical microscopy. Many of the materials that were known to be random copolymers or that were from the B group (B1 and B3) displayed typical spherulites, with Maltese cross corresponding to an optical birefringence when viewed through the polarized filter,[12] although not all were banded (Figure 9). Banding is generally accepted as being due to lamellar twisting[39,40] or to rhythmic crystal growth (discontinuity growth) of spherulites due to depletion of the polymer ahead of the growing crystal front in very thin films.[41] It is known that banding in PHB spherulites is affected by film thickness.[42]

For the samples in this study, volume-filling spherulites were observed when the polymers were allowed to crystallize at an

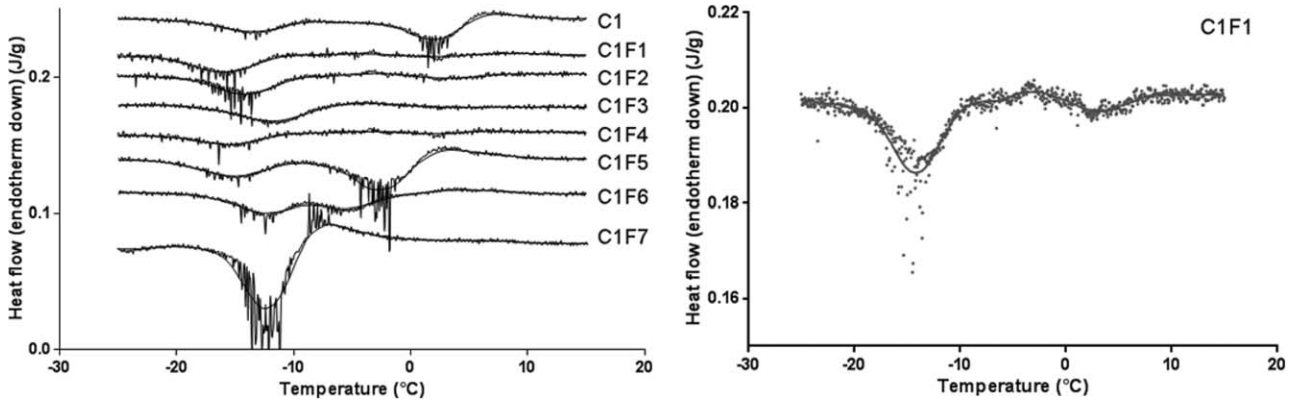

Figure 5. DSC thermograms showing first derivatives of T_gs of PHBV during the second heating scan for C1 and its fractions (left). Right-hand side: More detail of the first derivative of the T_g for C1 Fraction 1.

Table V. Avrami Parameters for PHBV Copolymers at Temperature of Fastest Crystallization, for As-Produced Materials, and Fractions

Sample	Fraction	T_{max} °C	n	k min^{-n}	$t_{1/2}$(expt'l) min	$t_{1/2}$(calc'd) min	T_m^0 °C	$\frac{1}{\gamma}$
A2	***Bulk***	40	2.63	0.000	82.3	81.1		
	1	40	1.68	0.132	2.6	2.7		
	2	40						
	3	40	2.62	0.000	82.3	85.2		
A4	***Bulk***	80	2.06	0.002	17.5	17.6		
	1	60	2.11	0.091	2.7	2.6	171.6	0.31
	2				Too slow			
	3	40	2.56	0.000	80.7	80.7		
B1	***Bulk***	70	1.95	0.003	17.4	16.9	~172	0.27
	1	60	2.09	0.047	3.7	3.6	179.1	0.32
	2				Too slow			
	3	20	1.70	0.003	24.7	24.6	118.7	0.47
B2	***Bulk***	90	1.79	0.005	15.8	16.5	175.6	0.33
	1	90	2.24	0.312	1.4	1.4	180.9	0.37
	2	40	1.73	0.002	32.2	31.1		
	3	40	1.70	0.002	29.6	28.7		
B3	***Bulk***	70	2.02	0.373	1.4	1.4	176.7	0.14
	1	80	1.92	5.448	0.4	0.3	175.2	0.23
	2	40	3.05	0.000	67.9	68.2		
C1	***Bulk***	70	2.07	0.087	3.0	2.7	176.2	0.17
	1	70	2.32	0.787	0.9	0.9	178.2	0.14
	2	70	1.86	1.112	0.8	0.8	171.1	0.17

appropriate temperature over a long enough time. The spherulite radius, *R*, increased linearly with time, consistent with Hoffman's theory, until the spherulites impinged on each other. For some of the as-produced random copolymeric materials that have been shown to be blends, we frequently observed distinct aprons where the crystalline morphology shifted with growth (Figure 9), presumably as different components within the system were being incorporated into the crystal in the later stages of crystallization that were not crystallizing in initially. At lower temperatures, there may also be some microphase separation in the crystals of these samples or simultaneous crystallization of two phases (Figure 9), but not for their fractions.

By contrast, the materials (including many of the respective fractions) that were designed to have blocky characteristics displayed very obvious phase separation within the spherulite (Figure 9). The effect of fractionation on the nominally block copolymeric material C1 was examined in more detail, comparing the as-produced material to the fractions from both the coarse and fine fractionations. The morphology of the fractions was distinctly different to that of the starting material (Figure 9). For the coarse fractionation, macrophase as opposed to microphase separation was observed in C1 Fraction 2. By contrast, for the fine fractions, there was still microphase separation within the spherulite for C1 Fine Fractions 1 and 4 but not for the other fine fractions.

The phase separation that was observed for the as-produced sample of C1 and the coarse Fraction 2 was likely due to blend incompatibilities rather than block copolymeric composition. The microphase separation seen in the fine Fractions 1 and 4 may also still be due to blends rather than the blocky nature of the material, and there may also be microcrystals (perhaps of PHB) forming in the early stages causing the inclusions evident in Figure 9. It is of interest although to note that the remaining fractions that showed no microphase separation still contained both high- and low-melting peaks in roughly equal proportions (~50–70% high melting as judged by the enthalpy of melting; Table IV). Therefore, the morphology observed is either due to the presence of blends, with the high-melting temperature components crystallizing independently first and the low-melting temperature components remaining in the interlamellar and interspherulitic spaces to crystallize slowly over time, or due to the block copolymers, which are able to pack effectively into a spherulite without phase separation evident on a microscopic scale. In semicrystalline block copolymers, it is known that higher order superstructure, such as spherulites, can coexist with a microphase-separated structure.[40] When the crystallizable block is the major component in a block copolymer, spherulites are usually formed as in the homopolymer.[43,44]

The mechanical properties of both C1 and C6 were distinctly different to the other as-produced samples. In particular, both had a much higher elongation to break, at 58% ± 19% and 49% ± 16% (mean ± 95% confidence interval), respectively, when compared with 5.0% ± 1.0% for all the other tested

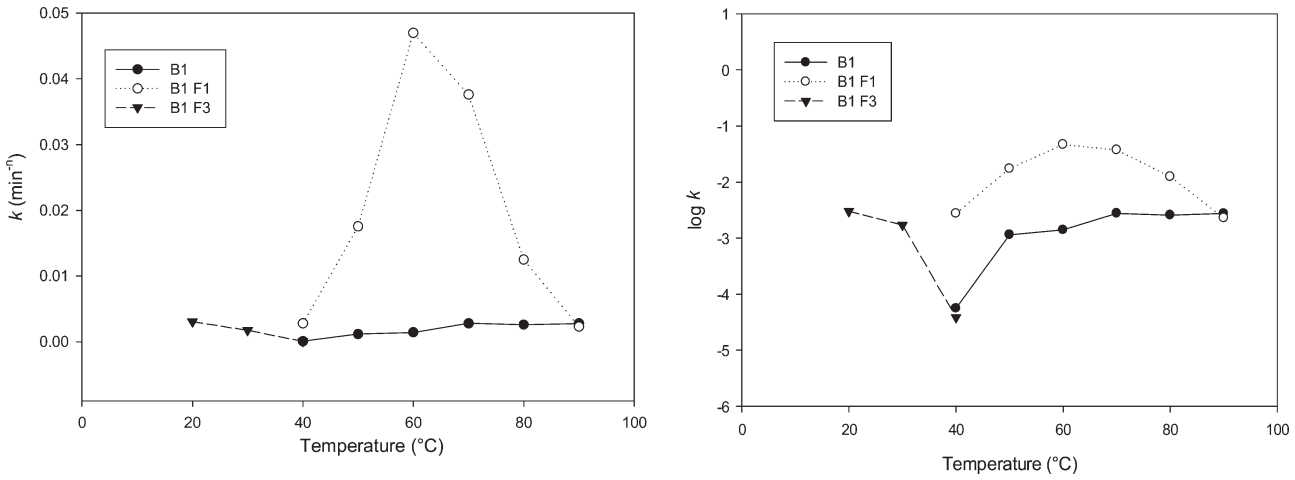

Figure 7. *k* values as determined from the Avrami plots for PHBV copolymer B1 (left) and the same data plotted as log *k* values against time (right).

samples. It is hypothesized that the distinctly different morphology evident for Sample C1 is associated with this difference in material properties.

Spherulitic Growth Kinetics

Spherulitic growth kinetics were analyzed in a similar fashion to our previous study,[12] with the crystalline growth rate (G) being

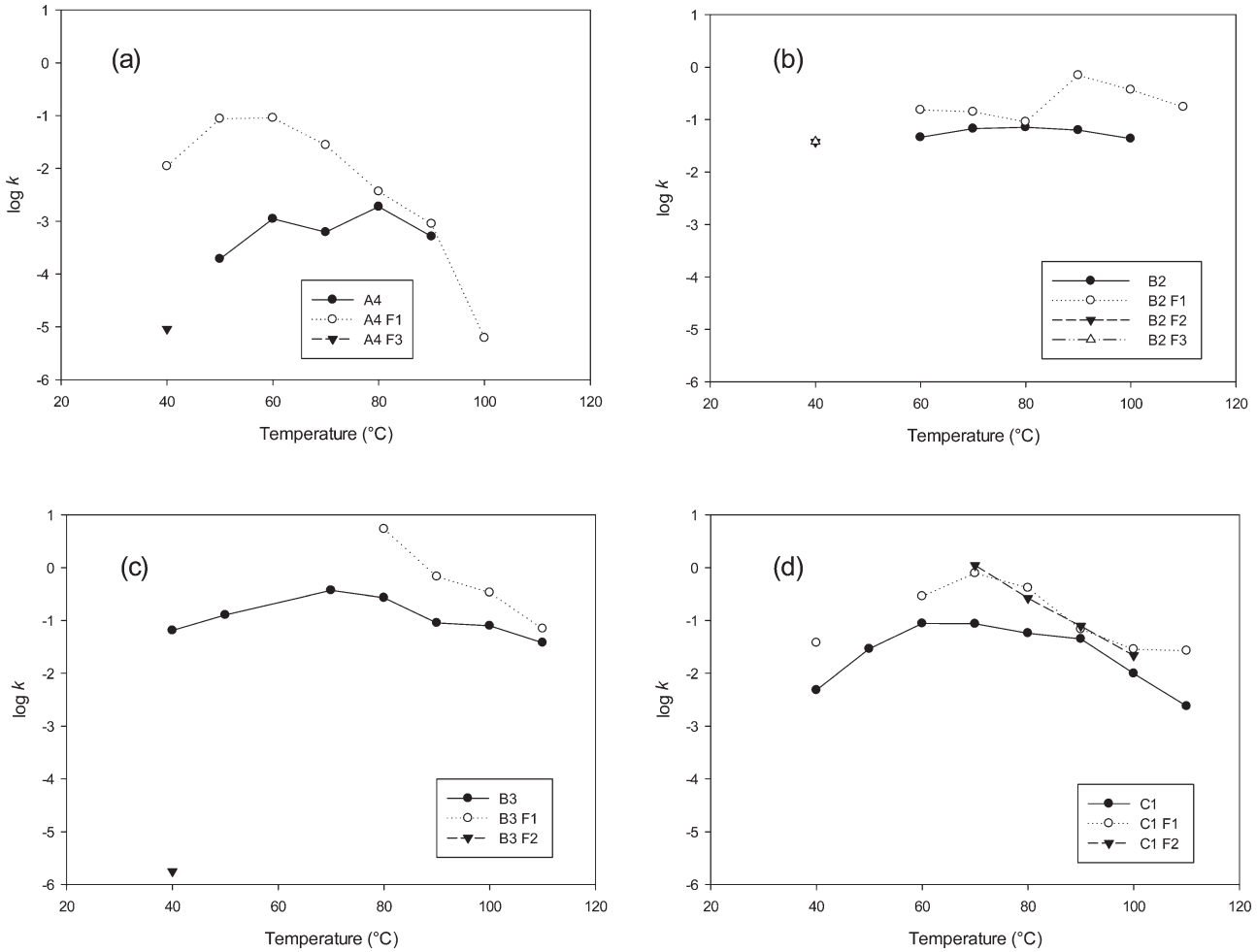

Figure 8. Log *k* values as determined from the Avrami plots for PHBV copolymer samples: (a) A4; (b) B2; (c) B3; and (d) C1.

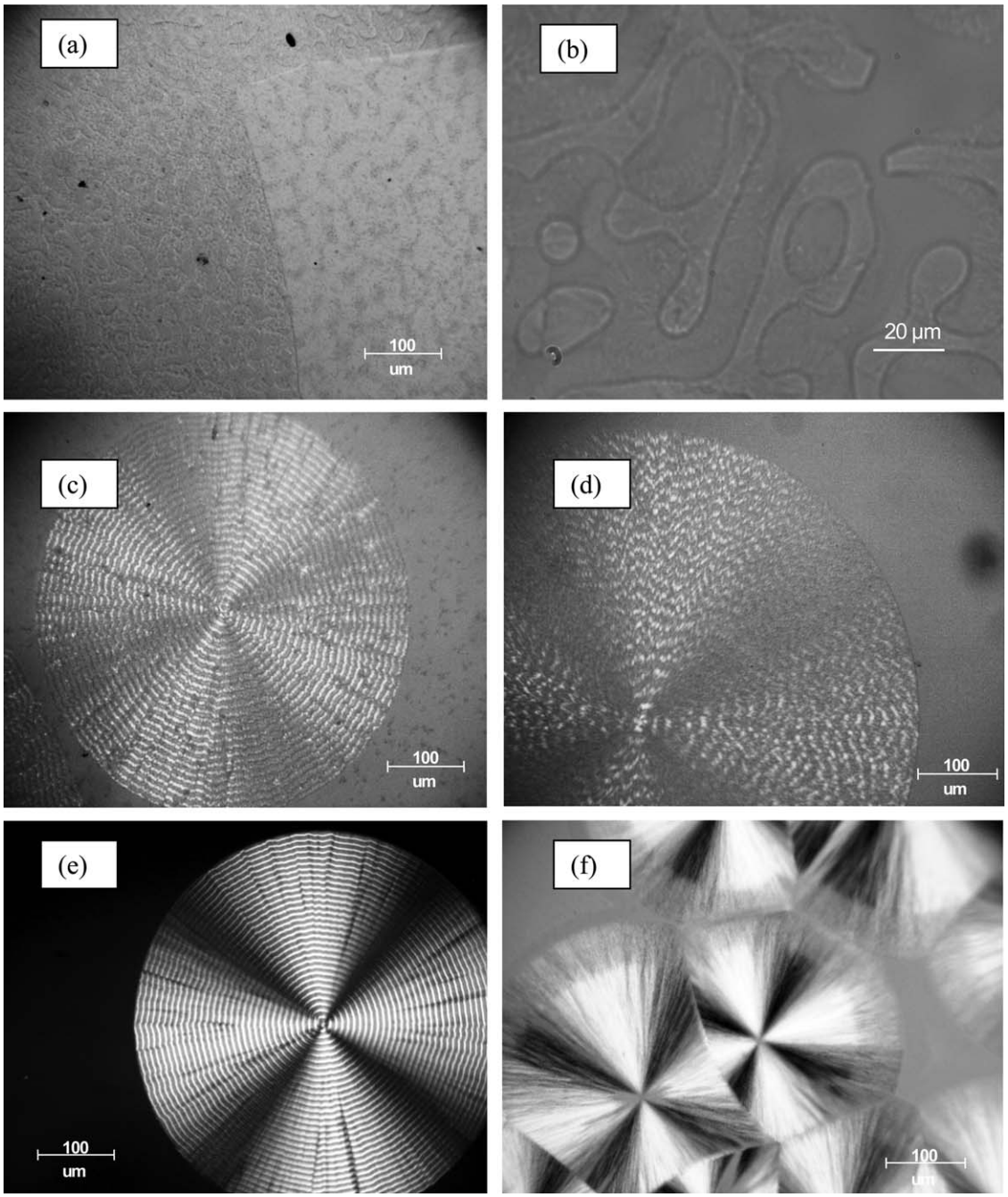

Figure 9. Polarized optical micrographs of PHBV copolymers: (a) C1 (as produced), isothermally crystallized at 70°C; (b) C1 Fraction 2 (coarse fractionation) at 90°C; (c) C1 Fraction 1 (fine fractionation) at 70°C; (d) C1 Fraction 2 (fine fractionation) at 70°C; (e) B2 Fraction 2 at 80°C; and (f) B2 (as produced) at 60°C.

calculated from the radial crystal growth in micrometers per second. Crystal growth curves for selected samples are given in Figure 10. As we observed from DSC assessment, the first fraction generally crystallized much faster than the as-produced material. By contrast, for Sample C1 (blocky copolymer, finely fractionated), Fractions 1 and 3 were fastest, with little difference between the other fractions.

Although the Avrami equation describes the overall isothermal crystallization behavior of polymers, the Lauritzen–Hoffmann model describing the growth of chain-folded polymer crystals [eq. (11)][45] is used to analyze the crystal growth behavior of linear flexible homopolymers and some semicrystalline/amorphous polymer blends that are crystallized from the melt[4646]:

$$G = G_0 \exp\left[-\frac{U^*}{R(T_{iso} - T_\infty)}\right] \exp\left[\frac{K_g}{T_c(\Delta T)f}\right], \qquad (11)$$

where G_0 is the preexponential factor, U^* is the activation energy for the transportation of crystallizable segments to the

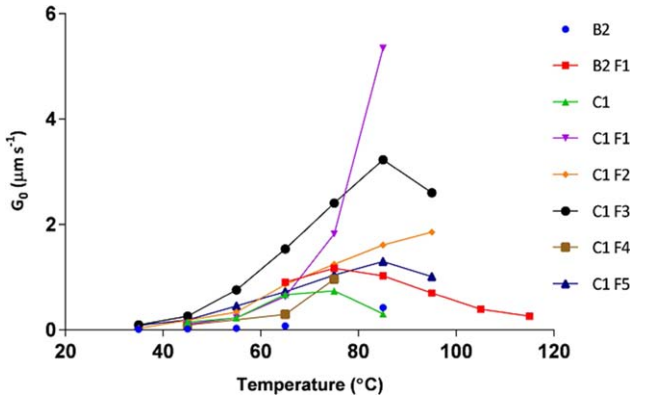

Figure 10. Radial growth rate (G) of PHBV spherulites at various crystallization temperatures (T_{iso}s) for copolymeric PHBV. [Color figure can be viewed in the online issue, which is available at wileyonlinelibrary.com.]

crystallization front, R is the gas constant (8.3145 J mol^{-1} K^{-1}), and T_∞ is a hypothetical temperature where all molecular motion-associated viscous flow ceases and is related to the T_g by $T_\infty = T_g - 51.6$ (K).[47] ΔT is the degree of supercooling given as $(T_m^0 - T_{iso})$, where T_m^0 is the equilibrium melting point. f is a factor that accounts for the variation in the enthalpy of fusion ΔH_f with temperature and is given by $f \approx 2T_c/(T_m^0 + T_{iso})$. K_g is the nucleation constant, which can be expressed as follows:

$$K_g = jb_0\sigma\sigma_e T_m^0 / \Delta H_f k, \quad (12)$$

where j may have the value 2 or 4 depending on the growth mechanism, b_0 is the layer thickness, σ and σ_e are the lateral and fold surface free energies of the growing crystal, respectively, and k is the Boltzmann's constant. The regime of crystallization for PHBV and its blends is assigned to be Regime III ($j = 4$) when T_{iso} is below 130°C (403 K),[48] and the growth rate data are plotted in the form of $\ln G + U^*/R(T_{iso} - T_\infty)$ against $1/(fT_{iso}\Delta T)$, where the slope is $-K_g$. The Williams–Landel–Ferry value for U^* of 17221.6 J mol^{-1} was used.[47]

In this case, there was a reasonable fit to the equation for most of the fractions (Figure 11), although this was not the case for

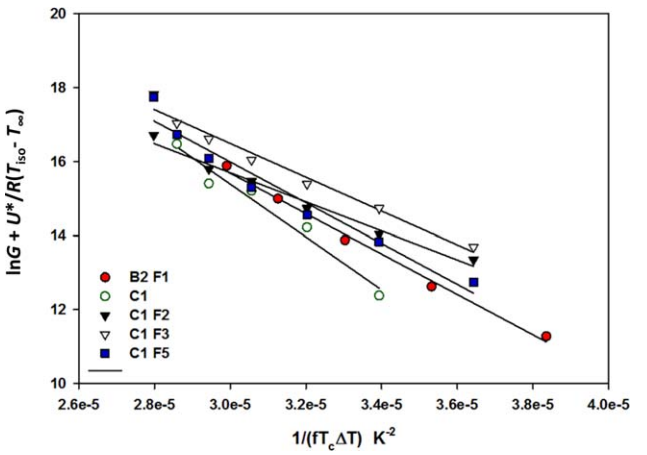

Figure 11. Lauritzen-Hoffman plot for selected PHBV copolymers (C1 as-produced, C1 F1, F3 and F5, and B2 F1). [Color figure can be viewed in the online issue, which is available at wileyonlinelibrary.com.]

Table VI. Spherulitic Growth Kinetic Parameters for PHBV Copolymers

Sample	K_g (10^5 K^2)	G_0 (μm s^{-1})	HV (mol %)
B2 Fraction 1	5.46	8.35E+13	64
C1	7.13	9.38E+15	43
C1 Fine Fraction 2	3.93	8.56E+11	30
C1 Fine Fraction 3	4.56	1.29E+13	34

Samples B2 and C1 Fine Fractions 1 and 4. This could possibly be because of microphase-related issues, where at the lower temperatures, competing crystallizations between low and high 3HV content crystalline phases may exist. The fit for the as-produced material C1 was also relatively poor (Figure 11), which is perhaps not surprising given the complex blend nature of this material. The values for K_g and G_0 determined from the curve fitting are given in Table VI.

These values are comparable with those in the literature, with $K_g = 4.79 \times 10^5$ for PHBV (2.6 mol % 3HV content),[49] 6.90×10^5 for PHB, and 7.67×10^5 for PHBV (14 mol % 3HV content).[36] The variation observed between fractions with similar 3HV contents could potentially be attributed to variations in the chain-folding regularities, as well as potential changes in block lengths contributing to variations in chain-packing ability. There was also some difference in molar mass, which could result in different degrees of interchain links and chain entanglements. All of these, in turn, could affect molecular motion in the melt and hence affect the degree of disorder in the intercrystalline region. Liu et al.[41] also observed that there was some variation in crystallization rate with variation in film thickness, which may partially account for the more minor variations observed between the fine fractions of C1.

It is not possible to convert these kinetic parameters to give an estimation of the lateral surface free energy in this study as we know from SAXS/WAXS analysis (not shown here) that both the 3HB and 3HV crystal units are commonly present in these materials and that the heat of fusion of an infinite crystal is also strongly dependent on 3HV content, with the values not yet being characterized for higher 3HV content PHBV.

CONCLUSIONS

In this work, we evaluated the compositional distribution of a broad range of as-produced bacterial PHBV's with widely differing 3HV contents and monomer unit distributions (from random to nominally blocky in character). All the materials were found to be composed of a very broad compositional distribution, with many containing a bimodal or multimodal copolymer composition, likely due to the fact that the biomass was enriched on a fermented whey waste that was low in propionic acid, in contrast to the feedstocks that were used for polymer production. The crystallization kinetics and morphology of the as-produced materials were found to be controlled by the most rapidly crystallizing fractions of lower 3HV content. In turn, the crystallization rate of the most rapidly crystallizing components

was significantly slower when present in a blend. However, the mechanism of crystallization, as judged by the Avrami constant (which averaged around 2.1 for all samples), was not significantly affected.

The two samples that had unique mechanical properties and that were produced using alternating feeding had thermal and crystallization properties that were consistent with a block copolymer and could not be fractionated into clearly separate random copolymers. Even with fine fractionation, most of the material retained both high- and low-melting components. The fractions were also among the fastest materials to crystallize, despite having 3HV contents of around 30–40 mol %. However, it is still not possible to be definitive with respect to the compositional distribution of these materials as morphological and NMR evidence is inconclusive.

Further work is also required to characterize the mechanical properties of the fractions, and thus the relationship of compositional, thermal, molar mass, and other properties to these properties. In addition, the effect of thermal rather than solvent processing of these materials needs to be evaluated.

ACKNOWLEDGMENTS

The authors thank the Australian Research Council for funding through grant ARC LP0990917. The ARC had no role in the study design, collection, analysis, or interpretation of the data. The authors also thank L. Karabegovic, P. Johansson, and P. Magnusson from AnoxKaldnes for their valuable assistance with pilot plant operation; Dr. Beatrice Keller-Lehman and Nathan Clayton for analytical analysis (UQ); and Dr. Tim Dargaville (QUT-IHBI) for analytical analysis.

REFERENCES

1. Laycock, B.; Halley, P.; Pratt, S.; Werker, A.; Lant, P. *Prog. Polym. Sci.* **2013**, *38*, 536.
2. Arcos-Hernandez, M. V.; Laycock, B.; Donose, B. C.; Pratt, S.; Halley, P.; Al-Luaibi, S.; Werker, A.; Lant, P. A. *Eur. Polym. J.* **2013**, *49*, 904.
3. Gurieff, N.; Lant, P. *Bioresour. Technol.* **2007**, *98*, 3393.
4. Anterrieu, S.; Quadri, L.; Geurkink, B.; Dinkla, I.; Bengtsson, S.; Arcos-Hernandez, M. V.; Alexanderson, T.; Morgan-Sagastume, F.; Karlsson, A.; Hjort, M.; Karabegovic, L.; Magnusson, P.; Johansson, P.; Werker, A. *N. Biotechnol.*, in press.
5. Kleerebezem, R.; van Loosdrecht, M. C. M. *Curr. Opin. Biotechnol.* **2007**, *18*, 207.
6. Johnson, K.; Jiang, Y.; Kleerebezem, R.; Muyzer, G.; van Loosdrecht, M. C. M. *Biomacromolecules* **2009**, *10*, 670.
7. Albuquerque, M. G. E.; Martino, V.; Pollet, E.; Averous, L.; Reis, M. A. M. *J. Biotechnol.* **2011**, *151*, 66.
8. Bengtsson, S.; Hallquist, J.; Werker, A.; Welander, T. *Biochem. Eng. J.* **2008**, *40*, 492.
9. Patel, M.; Gapes, D. J.; Newman, R. H.; Dare, P. H. *Appl. Microbiol. Biotechnol.* **2009**, *82*, 545.
10. Martinez-Sanz, M.; Villano, M.; Oliveira, C.; Albuquerque, M. G. E.; Majone, M.; Reis, M.; Lopez-Rubio, A.; Lagaron, J. M. *N. Biotechnol.*, in press; DOI: 10.1002/app.40333.
11. Wei, L.; Guho, N. M.; Coats, E. R.; McDaniel, A. G. *J. Appl. Polym. Sci.*, in press; DOI: 10.1002/app.40333.
12. Laycock, B.; Arcos-Hernandez, M. V.; Langford, A.; Pratt, S.; Werker, A.; Halley, P. J.; Lant, P. A. *N. Biotechnol.*, Available online 21 May 2013.
13. Yoshie, N.; Inoue, Y. *Int. J. Biol. Macromol.* **1999**, *25*, 193.
14. Yoshie, N.; Inoue, Y. *Macromol. Symp.* **2005**, *224*, 59.
15. Albuquerque, M. G. E.; Carvalho, G.; Kragelund, C.; Silva, A. F.; Barreto Crespo, M. T.; Reis, M. A. M.; Nielsen, P. H. *ISME J.* **2013**, *7*, 1.
16. Bloembergen, S.; Holden, D. A.; Hamer, G. K.; Bluhm, T. L.; Marchessault, R. H. *Abstr. Pap. Am. Chem. S* **1986**, *192*, 222.
17. Werker, A. G.; Bengtsson, S. O. H.; Karlson, C. A. B. (Inventors; Veolia Water Solutions & Tech, Alan Werker, Simon Bengtsson; Carl Karlsson assignees). Int. Pat. WO2011070544-A(2) (**2011**).
18. Werker, A. G.; Johannson, P. S. T.; Magnusson, P. O. G.; Maurer, F. H. J.; Jannasch, P. (Inventors; Veolia Water Solutions & Tech assignee). U.S. Pat. 2013203954-A(1) (**2013**).
19. Arcos-Hernandez, M. V.; Gurieff, N.; Pratt, S.; Magnusson, P.; Werker, A.; Vargas, A.; Lant, P. *J. Biotechnol.* **2010**, *150*, 372.
20. Dai, Y.; Lambert, L.; Yuan, Z. G.; Keller, J. *Process. Biochem.* **2008**, *43*, 968.
21. Žagar, E.; Krzan, A.; Adamus, G.; Kowalczuk, M. *Biomacromolecules* **2006**, *7*, 2210.
22. Kansiz Domínguez-Vidal, A.; McNaughton, D.; Lendl, B. *Anal Bioanal Chem.* **2007**, *388*, 1207–1213.
23. Watanabe, T.; He, Y.; Fukuchi, T.; Inoue, Y. *Macromol. Biosci.* **2001**, *1*, 75.
24. Feng, L. D.; Watanabe, T.; Wang, Y.; Kichise, T.; Fukuchi, T.; Chen, G. Q.; Doi, Y.; Inoue, Y. *Biomacromolecules* **2002**, *3*, 1071.
25. Yoshie, N.; Menju, H.; Sato, H.; Inoue, Y. *Macromolecules* **1995**, *28*, 6516.
26. Pomeranz, C. N.; Olesik, S. V. *J. Chromatogr. A* **2011**, *1218*, 7943.
27. Yu, F.; Nakamura, N.; Inoue, Y. *Polymer* **2010**, *51*, 4408.
28. Wang, Y.; Yamada, S.; Asakawa, N.; Yamane, T.; Yoshie, N.; Inoue, Y. *Biomacromolecules* **2001**, *2*, 1315.
29. Kamiya, N.; Yamamoto, Y.; Inoue, Y.; Chujo, R.; Doi, Y. *Macromolecules* **1989**, *22*, 1676.
30. Feng, L.; Yoshie, N.; Asakawa, N.; Inoue, Y. *Macromol. Biosci.* **2004**, *4*, 186.
31. Lemos, P. C.; Serafim, L. S.; Reis, M. A. M. *J. Biotechnol.* **2006**, *122*, 226.
32. Chen, C.; Fei, B.; Peng, S. W. *Eur. Polym. J.* **2002**, *38*, 1663.
33. Gunaratne, L. M. W. K.; Shanks, R. A. *Thermochim. Acta* **2005**, *430*, 183.
34. Akhtar, S.; Pouton, C. W.; Notarianni, L. *J. Polymer* **1992**, *33*, 117.
35. Organ, S. J.; Barham, P. J. *Polymer* **1993**, *34*, 2169.

36. Zhang, L. L.; Goh, S. H.; Lee, S. Y.; Hee, G. R. *Polymer* **2000**, *41*, 1429.

37. Bloembergen, S.; Holden, D. A.; Hamer, G. K.; Bluhm, T. L.; Marchessault, R. H. *Macromolecules* **1986**, *19*, 2865.

38. Ishida, K.; Asakawa, N.; Inoue, Y. *Macromol. Symp.* **2005**, *224*, 47.

39. Tanaka, T.; Fujita, M.; Takeuchi, A.; Suzuki, Y.; Uesugi, K.; Doi, Y.; Iwata, T. *Polymer* **2005**, *46*, 5673.

40. Xu, J.-T.; Liang, G.-D.; Fan, Z.-Q. *Polymer* **2004**, *45*, 6675.

41. Liu, J. P.; Qiao, X. P.; He, S. A.; Cao, Q. K.; Wang, H. *J. Appl. Polym. Sci.* **2010**, *115*, 1616.

42. Ashby, R. D.; Foglia, T. A.; Liu, C. K.; Hampson, J. W. *Biotechnol. Lett.* **1998**, *20*, 1047.

43. Floudas, G.; Tsitsilianis, C. *Macromolecules* **1997**, *30*, 4381.

44. Liu, L.-Z.; Xu, W.; Li, H.; Su, F.; Zhou, E. *Macromolecules* **1997**, *30*, 1363.

45. Hoffman, J. D.; Miller, R. L. *Polymer* **1997**, *38*, 3151.

46. Pearce, R. P.; Marchessault, R. H. *Macromolecules* **1994**, *27*, 3869.

47. Williams, M. L.; Landel, R. F.; Ferry, J. D. *J. Am. Chem. Soc.* **1955**, *77*, 3701.

48. Withey, R. E.; Hay, J. N. *Polymer* **1999**, *40*, 5147.

49. Shan, G. F.; Gong, X.; Chen, W. P.; Chen, L.; Zhu, M. F. *Colloid Polym. Sci.* **2011**, *289*, 1005.